

Influence of chemical structure of dyes, of pH and of inorganic salts on their photocatalytic degradation by TiO₂ comparison of the efficiency of powder and supported TiO₂

Chantal Guillard^{a,*}, Hinda Lachheb^{a,b}, Ammar Houas^b, Mohamed Ksibi^b,
Elimame Elaloui^b, Jean-Marie Herrmann^a

^a *Laboratoire d'Application de la Chimie à l'Environnement (LACE), Université Claude Bernard Lyon 1, 43 bd. du 11 November 1918, Bât Raulin, 3^{ème} étage, F-69622 Villeurbanne Cedex, France*

^b *Laboratoire de Catalyse et Environnement, Ecole Nationale d'Ingénieurs de Gabès (ENIG), Gabès, Tunisia*

Received 8 January 2003; accepted 14 January 2003

Abstract

Anionic (Alizarin S (AS), azo-Methyl Red (MR), Congo Red (CR), Orange G (OG)) and cationic (Methylene Blue (MB)) dyes were degraded, either individually or in mixtures, by using UV-irradiated TiO₂ in suspension or supported on glass and on paper. The influence of the chemical structure of different dyes as well as that of pH and of the presence of inorganic salts on the photocatalytic properties of TiO₂ has been discussed. The role of adsorption is suggested, indicating that the reaction occurs at the TiO₂ surface and not in the solution. S and N hetero-atoms are respectively mineralized into SO₄²⁻, NO₃⁻ and NH₄⁺, except azo-groups which mainly formed N₂ which represents an ideal case for a decontamination reaction. The fate of nitrogen strongly depends on its initial oxidation degree.

High photocatalytic activities have been found for TiO₂ coated on glass by the sol–gel method. Its efficiency was intermediate between those of PC-500 and P-25 powders.

The efficiency of PC-500 TiO₂ sample, fixed on paper by using a binder, is slightly less important than that of the powder. The presence of a silica-binder with an acidic pzc is suggested to be at the origin of the decrease in efficiency.

© 2003 Elsevier Science B.V. All rights reserved.

Keywords: Photocatalysis; Supported TiO₂; Dyes; Ions; pH; Solar energy

1. Introduction

Fifteen percent of the total world production of dyes is lost during the dyeing process and is released in textile effluents [1]. The release of those colored wastewaters in the ecosystem is a dramatic source of esthetic pollution, of eutrophication and of perturbations in the aquatic life. Wastewaters generated by the textile industries are known to contain considerable amounts of non-fixed dyes, especially of azo-dyes, and a huge amount of inorganic salts. It is well known that some azo-dyes and degradation products such as aromatic amines are highly carcinogenic [2]. Physical methods, such as adsorption [3], biological methods (biodegradation) [4,5] and chemical methods (chlorination, ozonation [6]) are the most frequently used for the treatment of these textile dyes. Other methods such as flocculation, reverse osmosis and adsorption on activated carbon have also

been tested [7–9]. The processes by bacterial beds are less adapted because of the fluctuations of the wastewater composition [10,11]. Since several years “Advanced Oxidation Processes” (AOP) have appeared. Among these processes, heterogeneous photocatalysis was found as an emerging destructive technology leading to the total mineralization of most of organic pollutants [12–19]. In most cases, the degradation is conducted for dissolved compounds in water with UV-illuminated TiO₂ powder.

The possible extents of the technique concern the irradiation source and the development and the use of TiO₂ supported. The great present interests are: (i) to use solar light which is free and inexhaustible, and (ii) to avoid the filtration which is an expensive process. Different studies were carried out to avoid this step by coating TiO₂ on many supports such as stainless steel [20], quartz [21], Pyrex [22], paper [23], fiberglass [24], clothes [25,26] and monolith [27,28].

The main drawback of coated TiO₂ is the decrease of its specific surface area [29,30].

* Corresponding author.

E-mail address: chantal.guillard@ec-lyon.fr (C. Guillard).

In the present article, it was attempted to determine the feasibility of the total degradation of some dyes used separately or in mixtures, by using photocatalysis in presence of powder or of supported TiO₂. TiO₂ was first supported on a non-woven paper of synthetic fiber prepared by Ahlstrom firm. Titania was also supported on glass in our laboratory by using a sol–gel method. The influence of pH and of inorganic salts was also determined.

2. Experimental

2.1. Materials

Degussa P-25 titanium dioxide was used as the reference photocatalyst. It is mostly in the form of anatase and has a BET surface area of 50 m²/g, corresponding to a mean particle size of ca. 30 nm. Millennium PC-500 titanium dioxide (100% anatase, specific surface area of 320 m²/g) or P-25 were coated on the non-woven paper made of synthetic fibers. The areal loading in TiO₂ was 27 g/m². TiO₂ coated on glass was prepared by sol–gel method by using 0.5 mol/l of isopropoxyde of titania in isopropanol. The support is dip-coated in the solution at a speed of 3.4 mm/s, dried at 150 °C during 1 h between each coating and then calcinated at 450 °C. The glass support was a cylinder of 8 cm diameter and 8 cm height. The amount of TiO₂ is about 3 mg/cm².

The five dyes were purchased from Fluka and used as received without further purification. Their solutions were prepared using water from a Millipore Waters Milli-Q purification unit. Their structures are given Table 1.

2.2. Apparatus

A reactor of 1 l was used in the laboratory experiments. It is equipped with a plunging tube in which a Philips HPK 125 W lamp was placed vertically. To avoid the heating of the solution, water was circulated through a cylindrical jacket, made of Pyrex and located around the plunging tube.

Two other photo-reactors were employed for solar experiments performed at the Solar Platform in Almeria (Spain) (Fig. 1):

- A new cascade falling film photo-reactor (called STEP) for all experiments performed with titania supported on non-woven inorganic fibers.
- A compound parabolic collector (CPC) photo-reactor for all experiments with TiO₂ in suspension.

Both solar photo-reactors were inclined with a 37° angle (Almeria local latitude) to get an optimum solar radiant flux around noon with a fixed rack.

The STEP photo-reactor was composed of 21 stainless steel stairs (stair height: 70 mm, stair width: 500 mm) covered with a 1 m² Pyrex sheet to strongly limitate water evaporation which could induce errors in concentrations. The deposited photocatalyst was laid on the 21 stairs of the STEP photo-reactor, which corresponded to a surface of 1.36 m² of non-woven material. The effluent flowed down on the steps before being collected in a tank, from which it was elevated to the top of the steps for recirculation.

The CPC photo-reactor has already been described elsewhere [31]. The configuration used was one module of eight Pyrex tubes (inner tube diameter: 48 mm, tube length: 3000 mm).

Table 1
Physicochemical characteristics of the dyes degraded

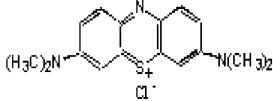
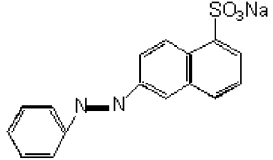
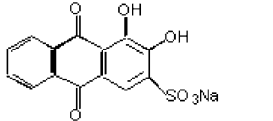
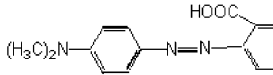
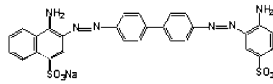
Dye	Chemical formula	M _w (g/mol)	λ _{max} (nm)	ε (l/(mol cm))
Methylene Blue (MB)		356	660	79.51 × 10 ³
Orange G (OG)		350.33	495	19.61 × 10 ³
Alizarin S (AS)		360.28	520	7.2 × 10 ³
Azo-Methyl Red (MR)		269.3	540	5.92 × 10 ³
Congo Red (CR)		696.68	510	18.67 × 10 ³



Fig. 1. Photo-reactors used at the Plataforma Solar de Almeria (Spain).

2.3. Procedure

2.3.1. Laboratory experiments

The volume of the aqueous solution of each dye introduced into reactor 1 was 750 ml, to which 375 mg of powder TiO_2 was added to get final concentration of 0.5 g/l. The same photo-reactor was used for titania coated on the glass support.

The degradations were carried out at 293 K and at different pH values. The pH was adjusted using either NaOH or HClO_4 . The suspension was first stirred in the dark for 60 min before irradiation to start the reaction at the adsorption equilibrium.

2.3.2. Solar experiments

The characteristics of CPC and STEP photo-reactors are given in Table 2. The amount of PC-500 used in CPC reactor is 0.5 g/l.

2.4. Analyses

A UV-Vis spectrophotometer “Safas Monaco 2000” was used for the determination of dye concentrations at the maximum of absorbance (Table 1).

Table 2
Characteristics of the CPC and STEP photo-reactors

	CPC photo-reactor	STEP photo-reactor
Effluent volume (l)	35	25
Activated volume (l)	13	11
Collector surface (m^2)	2	1
Flow rate (l/h)	1200	450

Anions and cations were analyzed by HPLC using a Waters 501 isocratic pump, a Waters 431 conductivity detector, and an IC-PAK HR anion column ($L = 50$ mm, i.d. = 4.6 mm, diameter of particules = 10 μm) or a Vydac Cation IC40 ($L = 50$ mm, i.d. = 4.6 mm). Eluents were respectively borate/gluconate at 0.9 ml/min and HNO_3 2.5 mM at 1.5 ml/min.

Total organic carbon (TOC) was determined by using a Bioritech (model 700) TOC analyzer. Chemical oxygen demand (COD) was measured using the acidic dichromate method with a Bioblock COD analyzer.

3. Results and discussion

3.1. Decolorization

The decolorization kinetics of the different dyes are given in Fig. 2. All reactions followed an apparent first-order kinetics, confirmed by the linear transforms $\ln C_0/C = f(t)$ illustrated in the insert in Fig. 2.

The rate constants of disappearance in min^{-1} are in the following order: azo-Methyl Red (MR) > Methylene Blue (MB) > Orange G (OG) \approx Alizarin S (AS) > Congo Red (CR). The smallest rate constant of CR can be explained by the steric hindrance of a large aromatic molecule which leads to a smaller number of CR molecule adsorbed on TiO_2 .

The higher degradability of MR could be due to the presence of a carboxylic group which can easily react with H^+ via a photo-Kolbe reaction whereas the presence of a withdrawing group, SO_3^- , is probably at the origin of the less efficient OG and AS degradations. Another suggestion to explain the difference of the reactivities of these different dyes could also be their ability to adsorption on TiO_2 as it can be seen on Fig. 3. This last hypothesis agrees with a reaction occurring at the surface of TiO_2 and not in the solution, close to the surface.

3.2. Influence of pH

Since dyes to be degraded can be at different pH values in real colored effluents, comparative experiments were performed at three pH values: 3, 6 and 9 (as presented in Fig. 4).

For all dyes, except for OG, the increase of pH favors their degradation. A study of their adsorption shows a similar behavior between adsorption and degradation, as showed in Fig. 4a and b. So it can be suggested that the influence of

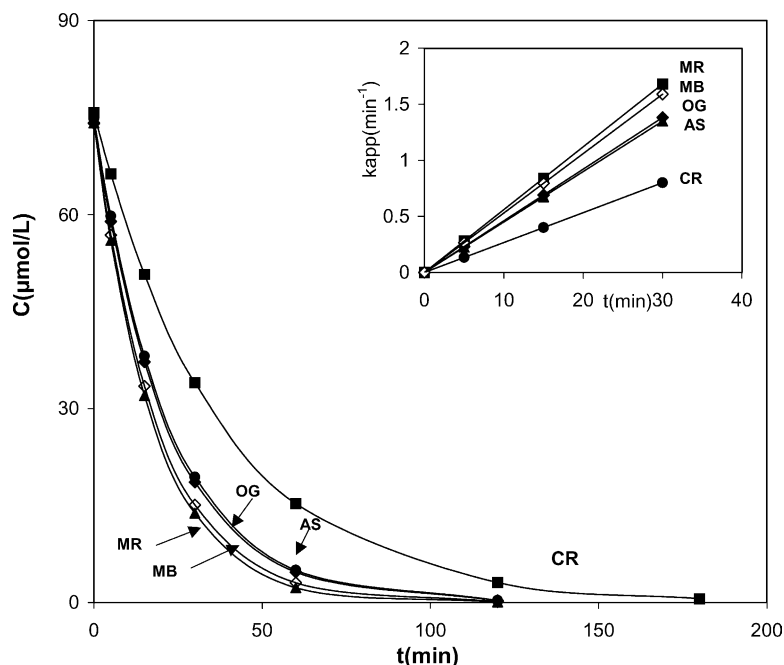
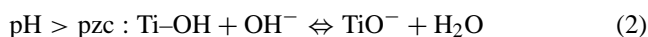


Fig. 2. Kinetics of the photocatalytic degradation of the dyes. In the insert: first-order linear transforms $\ln C_0/C = f(t)$. Conditions: $C_0 = 84.2 \mu\text{mol/l}$; $m(\text{TiO}_2) = 375 \text{ mg}$; $V = 750 \text{ ml}$; $T = 30^\circ\text{C}$; natural pH values.

pH on photocatalysis is due to the amount of dye adsorbed on TiO_2 .

The pH influences at the same time both the surface state of titania and the ionization state of ionizable organic molecules. For pH values higher than the pzc of titania, the surface becomes negatively charged and it is the opposite for $\text{pH} < \text{pzc}$, according to the following equilibria:



Since MB is a cationic dye (see Table 1), it is conceivable that at high pH values, its adsorption is favored on a negatively charged surface. By contrast, OG has its adsorption in-

hibited by high pH values because of its negatively charged sulfonate $-\text{SO}_3^-$ function. The other dyes, having several functional groups, have a resulting behavior similar to that of MB suggesting an adsorption on the OH or NH_2 groups.

The decrease of OG degradation at basic pH shows also that the formation of OH^\bullet by reaction between OH^- and H^+ , at basic pH, was not at the origin of the increase of the photocatalytic efficiency of the other dyes.

3.3. Influence of inorganic salts

In textile effluents huge amounts of inorganic salts are present with dyes. In the literature, the inhibition of photocatalytic properties in presence of ions is often explained by

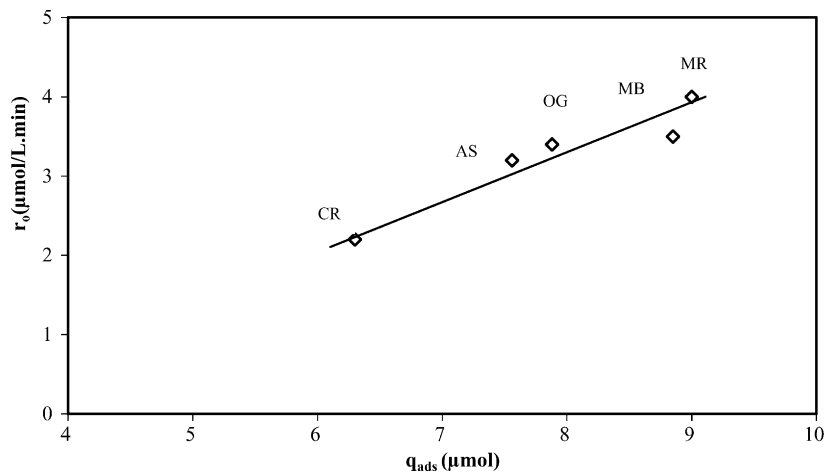


Fig. 3. Initial rate of MR, MB, OG, AS and CR disappearance as a function of the amount adsorbed.

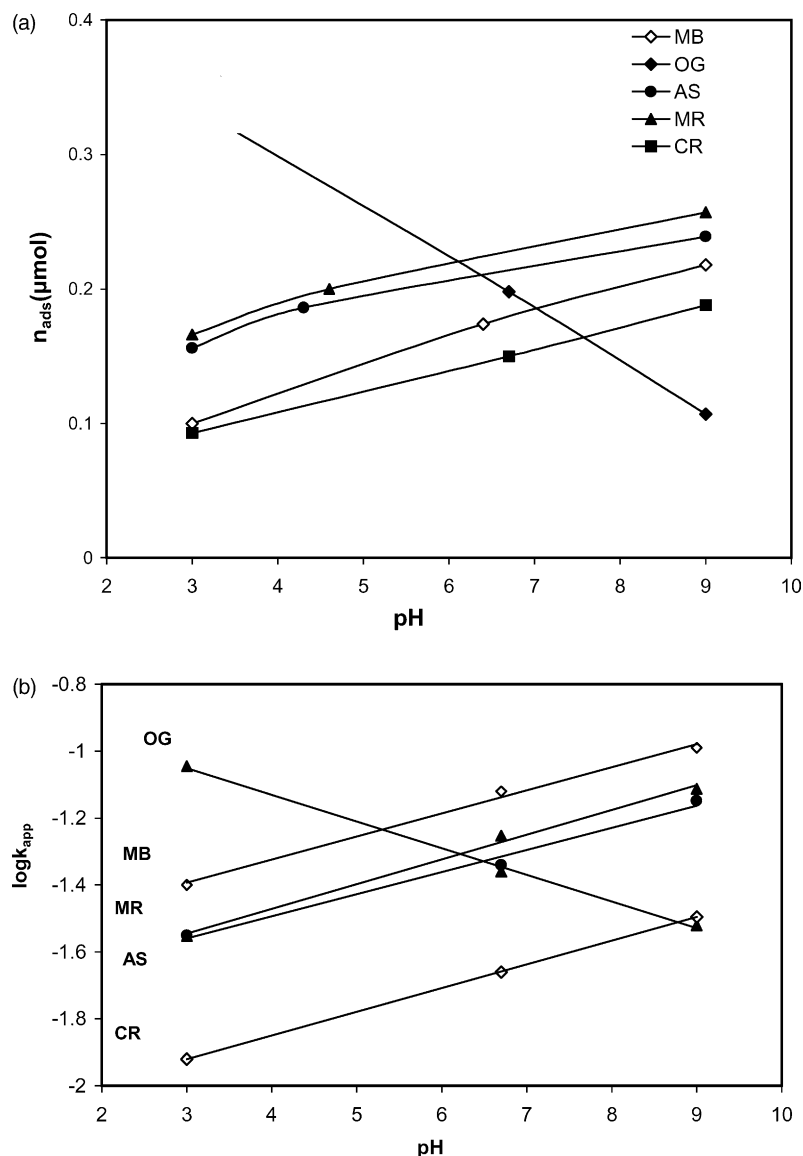
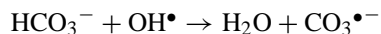
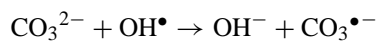


Fig. 4. Influence of pH on the amount of MB adsorption (a) and on the constant rate of MB photocatalytic disappearance (b).

the scavenging of OH^\bullet radicals by ions [17]. For example, the reaction of carbonate with OH^\bullet is given in the following equations:



The inhibition by inorganic salts of the degradation of MB at neutral and basic pH is in the following decreasing order:

carbonate > phosphate > sulfate > chloride > nitrate

In all cases, sodium salts have been used.

No correlation was found between the rate constant of ions with OH^\bullet radical (Table 3) and the order of inhibition of MB photodegradation, while a perfectly linear correlation was observed for MB between its adsorption at neutral or

basic pH and its initial rate of degradation (Fig. 5). This correlation can be explained by the formation of a double layer of salt at the surface of TiO_2 decreasing the adsorption of dyes. A more complete description of this phenomenon is still under study.

Table 3
Rate constants of ions with OH^\bullet radicals

Anions	Rate constants (l/(mol s))	References
NO_3^-	1.4×10^8	[36]
Cl^-	4.3×10^9	[37]
HCO_3^-	8.5×10^{-6}	[37]
CO_3^{2-}	3.9×10^8	[37]
SO_4^{2-}	1×10^{10}	[38]
HSO_4^-	3.5×10^5	[39]
H_2PO_4^-	$<10^6$	[40]

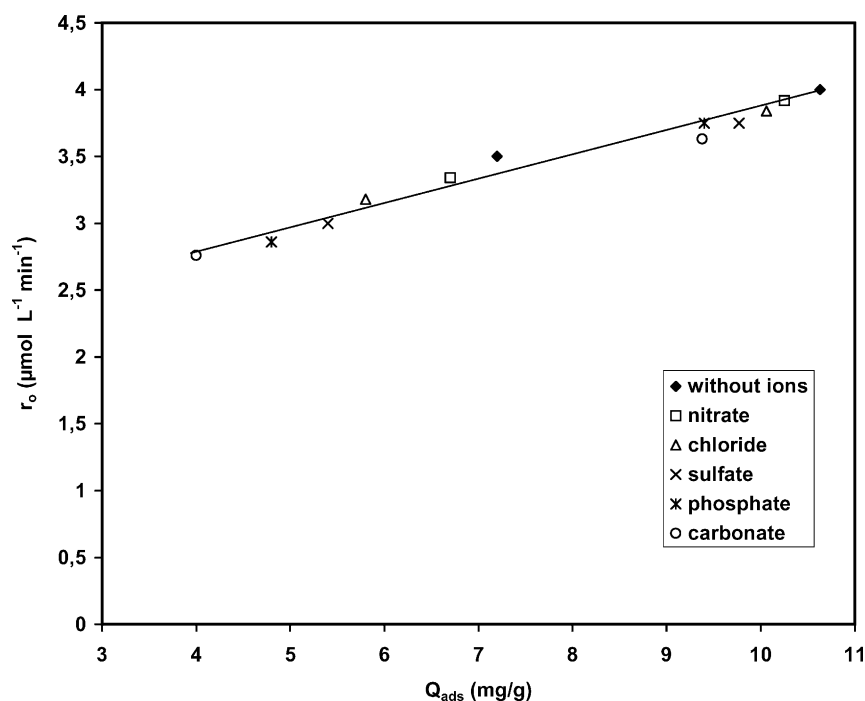


Fig. 5. Initial rate of MB disappearance as a function of MB adsorbed in presence of 2×10^{-2} mol/l of different inorganic sodium salts.

At basic pH, in presence of 2×10^{-2} mol/l of sodium carbonate, which is the most important inhibitor, a maximum inhibition of 9% only of the photocatalytic activity occurs, whereas a decrease of ca. 20% was observed at neutral pH. Moreover, at basic pH, the disappearance rate of MB in presence of 2×10^{-2} mol/l of sodium carbonate, is higher than that obtained at natural pH without addition of inorganic salt. Therefore, by modifying pH, the inhibiting effect of inorganic salt could be minimized.

3.4. Mineralization

3.4.1. TOC disappearance

The kinetics of TOC disappearance $[\text{TOC}] = f(t)$ are given in Fig. 6. It is shown that TOC has totally disappeared in less than 2 h for MR and in less than 6 h for CR. For the other dyes, the total organic carbon disappearance is complete after ca. 4 h of UV-irradiation. CR has the highest TOC disappearance rate probably in line with its highest number of carbon atoms ($n = 32$). However, the kinetics of TOC disappearance is not only fitted with the TOC amount. Whereas the number of carbon atoms of MR ($n = 15$) is situated between that of AS ($n = 14$) and that of OG or MB ($n = 16$), the photocatalytic degradability of MR is the highest. This can be explained by taking into account the carboxylic group of MR, ready for a first carbon atom elimination via a “photo-Kolbe” reaction resulting from the neutralization of the carboxylic group by a hole. Such easy reactions have already been observed for polycarboxylic [29] and butanoic [32] acids.

3.4.2. Hetero-atom mineralization

Two hetero-atoms are present in the dyes studied: sulfur and nitrogen atoms.

Sulfur was transformed into sulfate ion whereas nitrogen atoms produced ammonium, nitrate and nitrogen gas, given as follows.

3.4.2.1. Evolution of sulfate ions. Depending on the structure of the dyes, the initial rate of SO_4^{2-} formation varied in the following order: MB < CR < OG < AS (Table 4). This can be easily explained from the developed formulae in Table 1. AS has its sulfonyl group located on the dihydroxybenzene ring, more reactive through electrophilic reaction than the other parts of the molecule because of the presence of donor groups (OH). For OG, the sulfonyl group is linked to a less reactive naphthalenic aromatic ensemble.

The evolution of sulfate in CR (Table 4) is slow compared to that of OG, which has a similar structure but a higher number of carbon atom. Its low mineralization is probably due to the large size of the aromatic molecules, which decreases

Table 4
Initial appearance rate of sulfate ions, and percentage of sulfate evolved in the aqueous phase at the end of reaction

Dye	r_0 (SO_4^{2-}) ($\mu\text{mol}/(\text{l min})$)	Percentage SO_4^{2-} in solution
AS	7.5	100
OG	1	70
MB	0.2	60
CR	0.4	70

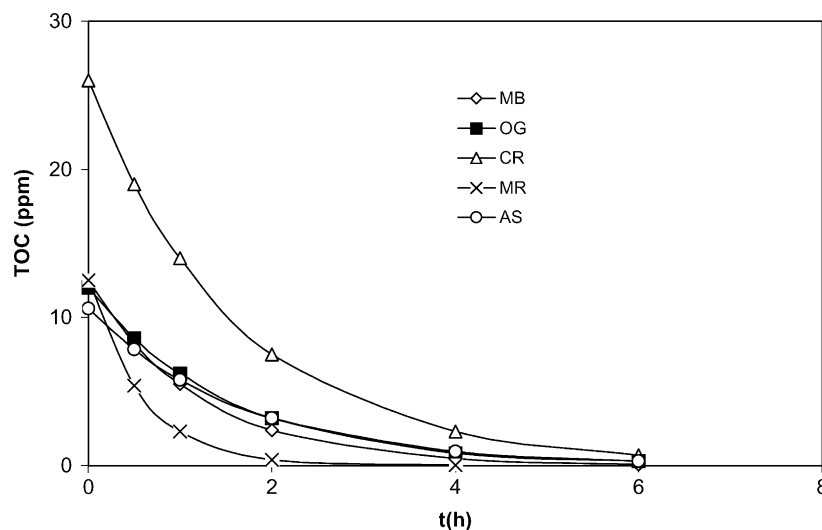


Fig. 6. Kinetics of TOC disappearance of five dyes at natural pH. Conditions: $C_{\text{dye}} = 84.2 \mu\text{mol/l}$; $V = 750 \text{ ml}$; $[\text{TiO}_2 \text{ P-25}] = 0.5 \text{ g/l}$; natural pH values.

the amount of CR adsorbed by nm^2 . Eventually, MB gives the lower rate in sulfate evolution. This is due to the fact that sulfur is involved in a $=\text{S}^+$ –aromatic link, yet less reactive. Additionally, sulfur is in the +4 oxidation state and not in the +6 one as in $\text{R}-\text{SO}_3^-$, thus requiring a two-electron oxidation process. Surprisingly, the sulfur-containing dyes did not release the expected stoichiometric quantities of sulfate. The exception of AS whose degradation released 100% sulfate ions could be tentatively correlated to the fact that AS is the only dye without nitrogen hetero-atom(s): the absence of transient NH_4^+ cations could favor a full evolution of sulfate into water.

3.4.2.2. Evolution of nitrogen-containing final products.

In all cases, the amount of NH_4^+ produced was always greater than NO_3^- . Except for MB, the other dye degradation did not provide any nitrogen mass balance in the aqueous phase. The fact that OG, MR and CR are diazoic dyes prompted us to perform GC analyses in a closed air-tight photo-reactor filled with pure oxygen. Increasing amounts of N_2 as a function of UV-irradiation time were measured until reaching the overall mass balance in nitrogen. Fig. 7 represents the evolution of NH_4^+ , NO_3^- and N_2 in the degradation of CR.

The fate of nitrogen strongly depends on its initial oxidation degree. When present in the -3 state as in amino groups, nitrogen spontaneously evolves as NH_4^+ cations with the same oxidation degree, before being subsequently and slowly oxidized into nitrate. In azo-dyes, both nitrogen atoms in the $-\text{N}=\text{N}-$ azo-groups are already formally at the zero oxidation degree. This oxidation degree close to zero combined with the existence of a $-\text{N}=\text{N}-$ double bond in the initial pollutant molecule favors the evolution of gaseous dinitrogen. N_2 evolution constitutes the ideal case for a decontamination reaction involving totally innocuous nitrogen-containing final product. The formation of N_2 has

already been observed by one of us in the degradation of triazolidine and triazole where $\text{N}-\text{N}$ or $\text{N}=\text{N}$ bonds are present [33].

3.5. Efficiency of TiO_2 powder to mineralize dye mixtures

Two mixtures of dyes (MR + CR) and (MB + OG) were tested with two different concentrations 42 and $84 \mu\text{mol/l}$. The TOC and DCO disappearance kinetics curves just fitted with the sum of TOC or DCO of both dyes degraded separately. Moreover, the TOC (or DCO) initial rate of the mixture is linearly link to the amount of TOC (or DCO). This means that the total coverage of TiO_2 by the dyes is not reached.

3.6. Efficiency of supported TiO_2

TiO_2 supported have been tested by using artificial light in laboratory experiments and solar light at Plataforma Solar de Almeria (Spain).

3.6.1. Laboratory experiments

Three samples of TiO_2 have been studied: two powders (P-25 and PC-500) and a sample of TiO_2 supported on glass and prepared by the sol–gel method.

Table 5 shows that supported TiO_2 prepared by the sol–gel method presents an efficiency comprised between those of

Table 5
Initial rate of sulfate formation in presence of different photocatalysts

Samples	r_0 ($\mu\text{mol}/(\text{l min g})$)
PC-500 powder	3
PC-500/glass (prepared by sol–gel)	5.1
P-25 powder	9.3

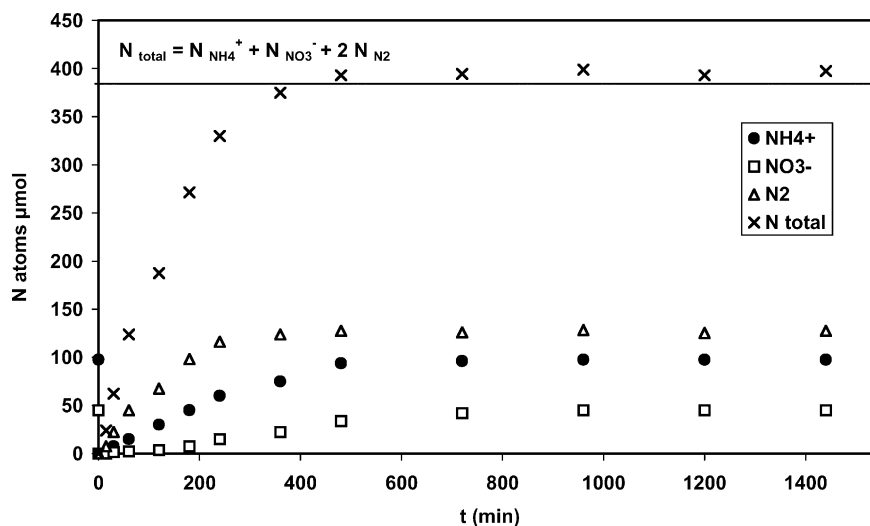


Fig. 7. Mass balance of nitrogen in Congo Red (CR) photocatalytic degradation.

PC-500 and P-25 powder. This result shows that the use of supported TiO_2 can be profitably envisaged to decontaminate wastewater with avoiding the final tedious filtration step, which strongly increases the overall cost of the treatment.

The important efficiency of TiO_2 supported on glass and prepared by sol-gel method is probably due to the presence of big agglomerates of cubic TiO_2 crystals of approximately 300 nm and a heterogeneous surface as observed by AFM (Fig. 8).

3.6.2. Experiment realized at the Plataforma Solar de Almeria

Congo red has been used to determine the efficiency of TiO_2 PC-500 coated on a non-woven paper using solar energy. Compared to the efficiency of a sample of PC-500 in powder, TiO_2 PC-500 supported on paper was found slightly less efficient as it can be seen in Fig. 9. However, a total decolorization was obtained after 4 h of irradiation.

To explain the smaller efficiency of industrial TiO_2 supported on a non-woven paper, two reasons can be suggested: (i) a competition of degradation between the pollutant and the paper, or (ii) the influence of the binder. The first reason can be eliminated because the photocatalytic activity of this industrial supported TiO_2 was found equivalent to that of TiO_2 powder when pesticides or 4-chlorophenol were degraded [34].

Therefore, the slightly less efficient activities of TiO_2 coated on non-woven paper can be attributed to the presence of a silica-binder added during the preparation. In the case of CR dye, the molecule was negatively charged. At $pH \approx 6.7$, the surface of TiO_2 is neutral. When TiO_2 is supported, the surface of SiO_2 used as a binder, is negatively charged (pzc of $SiO_2 \approx 2$). Therefore, the negatively charged surface decreases the adsorption of anionic compounds by electrostatic repulsion, and therefore decreases the photocatalytic activity. Actually a previous study on anisole has shown that

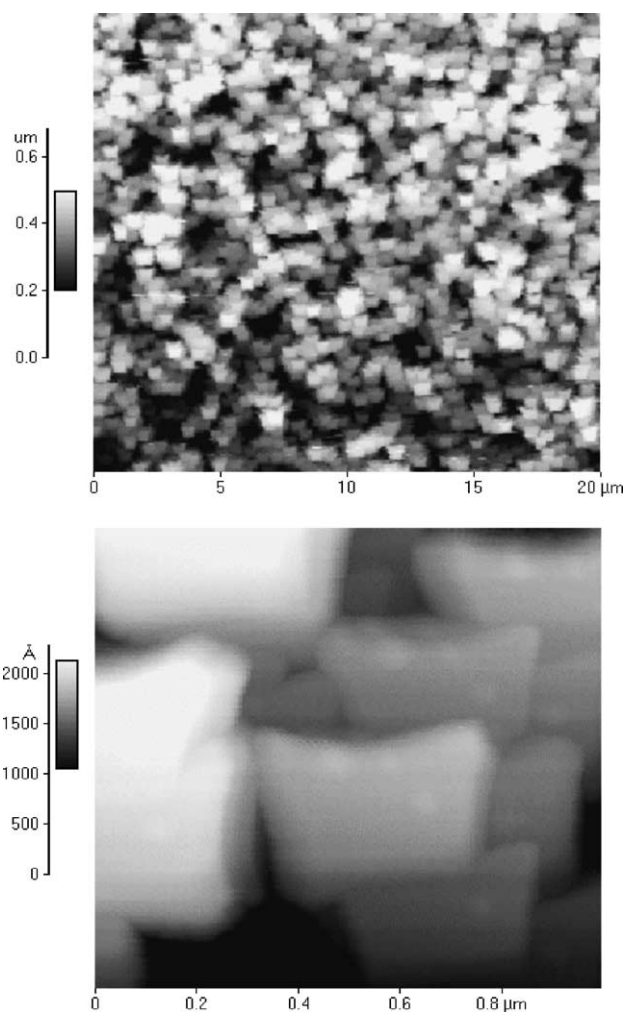


Fig. 8. AFM images of TiO_2 coated on glass: (A1) 20 μm × 20 μm; (A2) 1 μm × 1 μm × 1 μm.

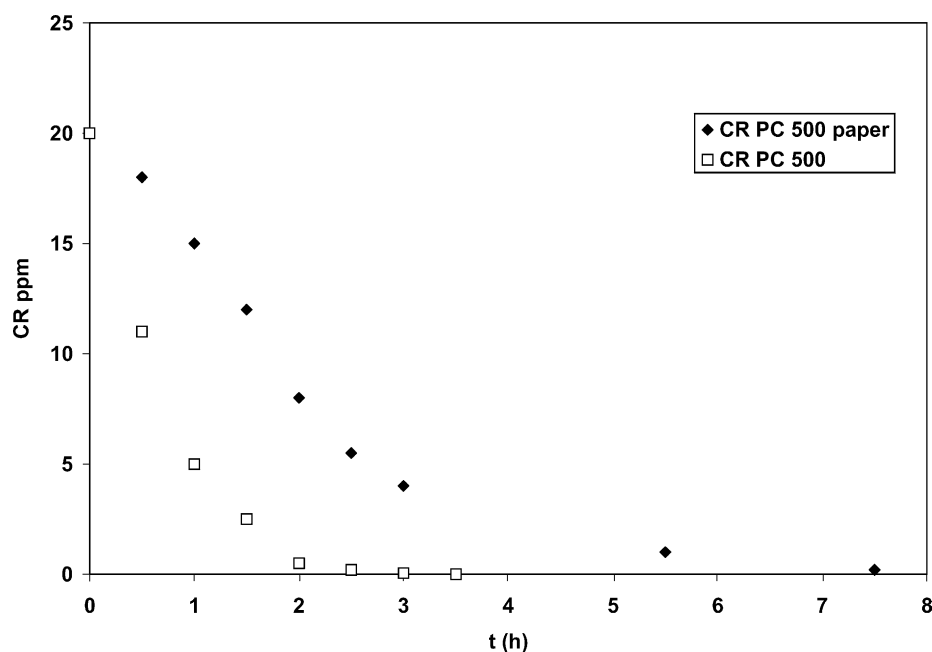


Fig. 9. CR disappearance, at the Plataforma Solar de Almeria (Spain) using supported PC-500 on paper or PC-500 powder with solar energy.

the photocatalytic degradation depended on the adsorption [35].

4. Conclusions

A direct correlation between the rate of degradation of dyes and their coverage at the surface of titania has been established. In addition to the influence of pH and of the presence of inorganic salts, this strongly suggests that the reaction essentially occurs in the adsorbed phase at the surface of TiO_2 and not in the solution as it has been sometimes claimed. The effect of inorganic salts has been attributed to the formation of a double layer of these salts, at the surface of TiO_2 , which inhibits the adsorption of dyes. The scavenging of OH^\bullet radicals by anions is not concerned in contrast to some previous works.

The study of the influence of pH on different structure has also permit to show that the formation of OH^\bullet by reaction between OH^- and H^+ , at basic pH, was not at the origin of the increase of the photocatalytic efficiency of the majority of organic compounds. The influence of pH also suggest that adsorption of ionic molecules occurs on the anionic part (COO^- or SO_3^-) only if there are no hydroxyl and amine groups.

The study of the hetero-atom mineralization has indicated that amino groups are mainly transformed into ammonium and subsequently into nitrate. By contrast, the azo-groups $-\text{N}=\text{N}-$ are mineralized into gaseous N_2 , totally innocuous for the environment. S atoms present either as sulfide ($=\text{S}^{+2}$) or as sulfonates (SO_3^-) are mineralized as sulfate.

The photocatalytic efficiency of TiO_2 coated on glass by sol-gel method has been found comparable to that of TiO_2

powder. This let us envisage to use such deposited to decontaminate wastewaters.

The smaller photocatalytic activity of TiO_2 supported on paper when compared to that of TiO_2 powder has been explained by the presence of a silica-binder whose low pzc induces repulsion of anionic dyes by electrostatic effects.

Acknowledgements

We thanks Ahlstrom Paper Group for the gift of samples of TiO_2 supported on paper.

References

- [1] H. Zollinger, *Color Chemistry: Synthesis, Properties and Applications of Organic Dyes and Pigments*, second revised ed., VCH, Weinheim, 1991.
- [2] M.A. Brown, S.C. De Vito, *Critical reviews in environmental science and technology* 23 (1993) 249.
- [3] (a) P.B. Dejohn, R.A. Hutchins, *Tex. Chem. Color* 8 (1976) 69; (b) A. Houas, I. Bakir, M. Ksibi, E. Elaloui, *J. Chem. Phys.* 96 (1999) 479.
- [4] S.S. Patil, V.M. Shinde, *Environ. Sci. Technol.* 22 (1988) 1160.
- [5] A.T. More, A. Vira, S. Fogel, *Environ. Sci. Technol.* 23 (1989) 403.
- [6] Y.M. Slokar, A.M. Le Marechal, *Dyes Pigments* 37 (1998) 335.
- [7] P.J. Halliday, S. Beszedits, *Can. Textile J.* 103 (1986) 78.
- [8] G.S. Gupta, G. Prasad, V.N. Singh, *Water Res.* 24 (1990) 45.
- [9] K.R. Ramakrishn, T. Viraraghavan, *Water Sci. Technol.* 36 (1997) 189.
- [10] R.H. Horning, *Textile Chem. Colorist* 9 (1997) 24.
- [11] U. Pagga, D. Brown, *Chemosphere* 15 (1986) 479.
- [12] J.-M. Herrmann, *Water treatment by heterogeneous photocatalysis*, in: F. Jansen, R.A. van Santen (Eds.), *Environmental Catalysis, Catalytic Science Series*, vol. 1, Imperial College Press, London, 1999, Chapter 9, pp. 171–194.

- [13] M. Schiavello (Ed.), *Photocatalysis and Environment: Trends and Applications*, Kluwer Academic Publishers, Dordrecht, 1988.
- [14] N. Serpone, E. Pelizzetti (Eds.), *Photocatalysis: Fundamentals and Applications*, Wiley/Interscience, New York, 1989.
- [15] J.-M. Herrmann, C. Guillard, P. Pichat, *Catal. Today* 17 (1993) 7.
- [16] H.A. Al-Ekabi, D. Ollis (Eds.), *Photocatalytic Purification and Treatment of Water and Air*, Elsevier, Amsterdam, 1993.
- [17] D.W. Bahnemann, J. Cunningham, M.A. Fox, E. Pelizzetti, P. Pichat, N. Serpone, in: R.G. Zeep, G.R. Helz, D.G. Crosby (Eds.), *Aquatic Surface Photochemistry*, Lewis Publishers, Boca Raton, 1994, p. 261.
- [18] O. Legrini, E. Oliveros, A.M. Braun, *Chem. Rev.* 93 (1993) 671.
- [19] D.M. Blake, *Bibliography of Work on the Photocatalytic Removal of Hazardous Compounds from Water and Air*, NREL/TP-430-22197, National Renewable Energy Laboratory, Golden Co., 1997.
- [20] U. Stafford, K.A. Gray, P.V. Kamat, A. Varma, *Chem. Phys. Lett.* 205 (1993) 55.
- [21] N.N. Lichtin, M. Avudaithai, E. Berman, J. Dong, *Res. Chem. Intermed.* 20 (1994) 755.
- [22] S.A. Larson, J.A. Widegren, J.L. Falconer, *J. Catal.* 157 (1995) 611.
- [23] H. Matsubara, M. Takada, S. Koyama, K. Hashimoto, A. Fujishima, *Chem. Lett.* 9 (1995) 767.
- [24] D.Y. Goswami, D.M. Trivedi, S.S. Block, *J. Sol. Energy Eng.* 119 (1997) 92.
- [25] C. Shifu, C. Xueli, T. Yaowu, Z. Mengyue, *J. Chem. Technol. Biotechnol.* 73 (1998) 264.
- [26] J.S. Kim, I.K. Toh, M. Murabayashi, B.A. Kim, *Chemosphere* 38 (1999) 2969.
- [27] R.J. Hall, P. Bendfeldt, T.N. Obee, J.J. Sangiovanni, *J. Adv. Oxidation Technol.* 3 (1998) 243.
- [28] M.L. Sauer, D.F. Ollis, *J. Catal.* 158 (1996) 570.
- [29] X. Fu, L.A. Clark, W.A. Zeltner, M.A. Anderson, *J. Photochem. Photobiol. A: Chem.* 97 (1996) 181.
- [30] I. Sopyan, M. Watanabe, S. Murasawa, K. Hashimoto, A. Fujishima, *J. Photochem. Photobiol. A: Chem.* 98 (1996) 79.
- [31] S. Malato, J. Blanco, J.-M. Herrmann, *Catal. Today* 54 (1999).
- [32] C. Guillard, *J. Photochem. Photobiol. A: Chem.* 135 (2000) 65.
- [33] C. Guillard, S. Horikoshi, N. Watanabe, H. Hidaka, P. Pichat, *J. Photochem. Photobiol. A: Chem.* 149 (2002) 155.
- [34] H. Lachheb, E. Puzenat, A. Houas, M. Ksibi, E. Elaloui, C. Guillard, J.-M. Herrmann, *Appl. Catal. B: Environ.* 39 (2002) 75.
- [35] L. Amalric, C. Guillard, E. Blanc-brude, P. Pichat, *Water Res.* 30 (1996) 1137.
- [36] Y. Katsumura, *J. Phys. Chem.* 95 (1991) 4435.
- [37] G.V. Buxton, C.L. Greenstock, W.P. Helman, A.B. Ross, *J. Phys. Chem. Data* 17 (2) (1988) 513–780.
- [38] J. Holcman, T. Logager, K. Sehested, V. Klaning, *Laboratory Studies on Atmospheric Chemistry*, New York, 23–25 September 1991, p. 41.
- [39] B. Lesigne, C. Ferradini, J. Pucheault, *J. Phys. Chem.* 76 (1972) 24.
- [40] J.K. Thomas, *Trans. Faraday Soc.* 61 (1965) 1324.